Anharmonicity changes the solid solubility of a random alloy at high temperatures — supplementary information

Nina Shulumba,[1,2] Olle Hellman,[3,1] Zamaan Raza,[1] Björn Alling,[1,4] Jenifer Barrirero,[2,1] Frank Mücklich,[2] Igor A. Abrikosov,[1,5] and Magnus Odén[1]

[1] *Department of Physics, Chemistry, and Biology (IFM), Linköping University, SE-581 83, Linköping, Sweden.*
[2] *Functional Materials, Saarland University, Campus D3 3, D-66123 Saarbrücken, Germany.*
[3] *Division of Engineering and Applied Science, California Institute of Technology, Pasadena, California 91125.*
[4] *Max-Planck-Institut für Eisenforschung GmbH, D-40237 Düsseldorf, Germany*
[5] *Materials Modeling and Development Laboratory, NUST "MISIS", 119049 Moscow, Russia.*

(Dated: September 29, 2016)

NOMENCLATURE

Table I summarises the acronyms and approximations used.

List of Acronyms		
Acronym	Description	Summary
SMD-HA	Small displacement method (harmonic approximation)	Free energy is calculated using force constants and volume at 0 K
SIFC-HA	Symmetry imposed force constants (harmonic approximation)	Free energy is calculated using force constants computed at 300 K, with 0 K volume
SIFC-QHA	Symmetry imposed force constants (quasi-harmonic approximation)	Free energy is calculated using force constants computed at 300 K and includes thermal expansion
SIFC-TDEP	Symmetry imposed force constants temperature dependent effective potential method	Free energy is calculated using temperature dependent interatomic force constants and thermal expansion
UP-TILD	Upsampled thermodynamic integration using Langevin dynamics (UP-TILD) approach [1]	Implementation of thermodynamic integration using Langevin dynamics
SQS	Special quasirandom structure [2]	Method for generating a substitutionally disordered systems (alloy)

TABLE I. Acronyms and their description

METHODOLOGICAL DETAILS

In order to find the effective force constant matrix that best represents the Born-Oppenheimer potential energy surface, we minimize the difference in forces between the model system and the SQS model of a real alloy, computing the latter by means of *ab initio* molecular dynamics (AIMD). We seek the linear least squares solution for the force constants $\bar{\bar{\Phi}}_{ij}^{\text{eff}}$ that minimize the difference in forces $\Delta\mathbf{F}$ between AIMD and our Hamiltonian form $\{\mathbf{F}_t^{\text{m}}\}$.

$$\begin{aligned}\min_{\bar{\bar{\Phi}}} \Delta\mathbf{F} &= \frac{1}{N_t}\sum_{t=1}^{N_t}\left|\mathbf{F}_t^{\text{MD}} - \mathbf{F}_t^{\text{H}}\right|^2 \\ &= \frac{1}{N_t}\sum_{t=1}^{N_t}\left|\mathbf{F}_t^{\text{MD}} - \bar{\bar{\Phi}}^{\text{eff}}\mathbf{U}_t^{\text{MD}}\right|^2,\end{aligned} \tag{1}$$

where $\{\mathbf{U}_t^{\text{MD}}\}$ and $\{\mathbf{F}_t^{\text{MD}}\}$ are sets of displacements and forces from AIMD respectively. TDEP potential energy surface is given by

$$U_{\text{TDEP}}(t) = U_0(t) + \frac{1}{2}\sum_{ij}\mathbf{u}_i(t)\bar{\bar{\Phi}}_{ij}^{\text{eff}}(t)\mathbf{u}_j(t), \tag{2}$$

where $\mathbf{u}_{i,j}$ are displacement of atoms i, j respectively and t is time. U_0 is a non-harmonic term, containing the renomalized baseline for the TDEP quasiparticles. It is determined from the criteria that the average potential energy from MD and TDEP should be equal:

$$U_0(T) = \left\langle U_{\text{MD}}(t) - \frac{1}{2}\sum_{ij}\mathbf{u}_i(t)\bar{\bar{\Phi}}_{ij}^{\text{eff}}(t)\mathbf{u}_j(t)\right\rangle, \tag{3}$$

where the brackets indicate a configuration (time) average at temperature T. The U_0 contains all the difference between 0 K and finite temperatures potential energies Fig. 1. To extract only the non-harmonic renormalization term we take the difference between between 0 K energies and calculated U_0 in eq. (3):

$$\Delta U_0(T) = U_0(T) - U_{el}. \tag{4}$$

This term later is added to the vibrational free energy in Eq. (3) in the main text.

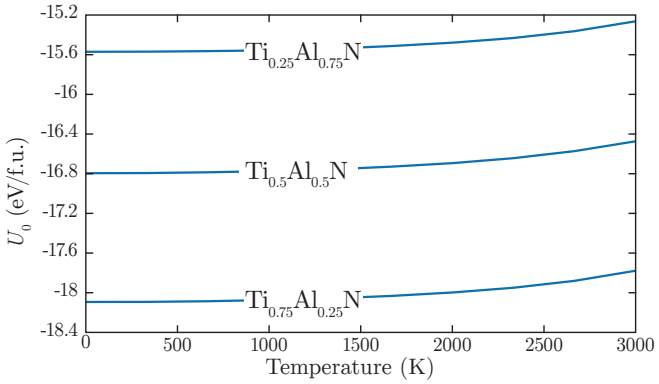

FIG. 1. (Color online) U_0 as a function of temperature for different concentrations of alloy.

COMPUTATIONAL DETAILS

Ab initio molecular dynamics

Canonical ensemble *ab initio* molecular dynamics simulations were performed using the projector-augmented wave (PAW) method [3] as implemented in VASP[4–7] over a range of temperatures, volumes, and concentrations. The temperature was set with a Nosé thermostat [8] with Fermi smearing corresponding to the simulation temperature. The plane wave energy cutoff was set to 600 eV and the Brillouin zone (BZ) was sampled at the Gamma point. The random alloy was generated using a special quasirandom structure (SQS) approach [2]. A 128 atom SQS ($4 \times 4 \times 4$) supercell was constructed, in which 64 atoms were metal and 64 were nitrogen. Three different SQS were generated, corresponding to different compositions of the random $Ti_{1-x}Al_xN$ alloy, with B1 symmetry and x={0.25,0.5,0.75}. 128 atoms SQS was generated to mimic the SRO parameters of perfect random alloys for the first 7 coordination shells for pair interactions with extra focus on the first 5. The small-radius 4 and 3-site clusters where taken into account, but focus was on pairs. For Al-rich compositions all configurational interactions become strong, but the short range 2-site interactions give the largest contribution to the energy. We assume that the vibrational free energy shows a qualitatively similar dependence with respect to energy on 2-site correlation functions as it does with 3- and 4-site functions.

The SQS were optimized at zero kelvin, to allow for local relaxations. Displacements from equilibrium positions during MD simulations were computed relative to these relaxed equilibrium positions.

A subset of uncorrelated samples from the AIMD simulations was selected and upsampled to high accuracy with a $3 \times 3 \times 3$ k-point mesh [9] for the BZ integration. The effective force constants where found to be smooth and easily interpolated across the whole concentration interval, giving the phonon DOS as a continuous function of concentration, volume and temperature.

Thermodynamic integration

Phase stability at constant temperature and volume is determined by the Helmholtz free energy F [10], where U_m and U are potential energies of model and real system respectively.

$$F = F_m + \underbrace{\int_0^1 \langle U - U_m \rangle_\lambda \, d\lambda}_{\Delta F}. \tag{5}$$

Equation 5 is formally exact for phase equilibria in alloys at relevant temperatures. In practice, calculating ΔF can be very difficult [1], so our strategy will be to choose the model system with the force constants that minimise ΔF. Ideally, it should be within the error bars of *ab initio* calculations.

Thermodynamic integration was used to validate our choice of Hamiltonian, but we emphasize that it is a benchmark, and not part of the SIFC-TDEP method. A Langevin thermostat was used to control the temperature and break the mode-locking. The numerical integration over coupling parameter λ was carried out over 5 discrete steps, and the MD simulations were run for ∼100 000 timesteps with k-point sampling at the Γ point only. A set of uncorrelated snapshots was selected from AIMD and upsampled to high accuracy with a $3 \times 3 \times 3$ k-point mesh to ensure convergence for ΔF.

PHONON DENSITY OF STATES

The phonon density of states was integrated on a $27 \times 27 \times 27$ q-point grid using the tetrahedron approach [11], ensuring convergence of the phonon free energy (F_{vib}) to within 0.01 meV/atom. In our case the dramatic difference in phonon free energy comes directly from anharmonic behaviour of phonon density of states. The low frequency part (see Fig. 2) contributes most to the shift in the free energy at high temperatures.

Benchmark test

We perform a series of additional calculations to check the reliability of our method. Using the small displacement method, the harmonic vibrational Gibbs free energy was calculated for the full SQS, treating all atoms as non-equivalent and thus including local environment effects in the force constants. This was compared to the SIFC-TDEP vibrational Gibbs free energy (Fig. 1 in the main text). Harmonic phonon free energies are

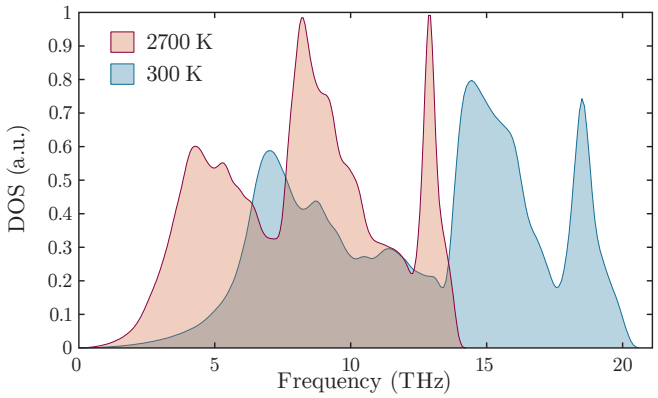

FIG. 2. (Color online) Phonon density of states for 300 K and 2700 K including thermal expansion and anharmonic effects using SIFC-TDEP method.

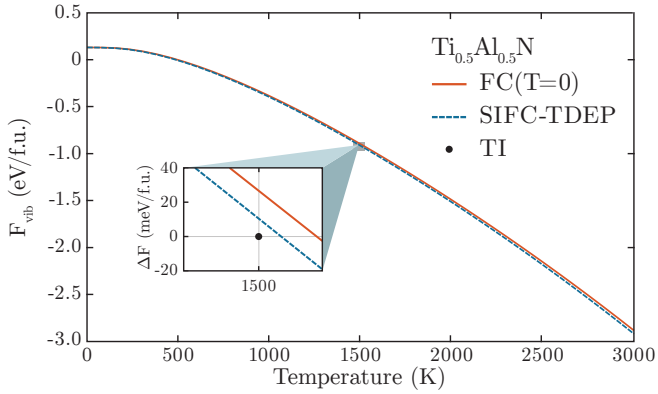

FIG. 3. (Color online) Phonon free energy as a function of temperature at constant volume. Harmonic free energy calculated with force constants extracted at 0K using small displacement method (red solid line). Harmonic free energy calculated using SIFC-TDEP with the force constants and ΔU_0 at the same volume (1500 K) is shown by blue dashed line. Free energy calculated by upsampled thermodynamic integration using Langevin dynamics is shown as the black point. We include the insert showing the difference between mentioned above free energies at 1500 K taking the thermodynamic integration point as a reference.

compared at a specific concentration ($Ti_{0.5}Al_{0.5}N$) and volume/atom (9.1260 Å^3). For the small displacement method, force constants are taken at zero temperature, while "SIFC-TDEP" denotes a free energy calculated using SIFC-TDEP force constants. At high temperature, the harmonic approximation is no longer a good benchmark, even at constant volume. In this case, we benchmarked using UP-TILD, which is formally exact in that region. Fig. 3 shows the comparison of the phonon free energies at the same volume taken at 1500 K. The free energy calculated using temperature-dependent force constants and the anharmonic correction (ΔU_0) lies closer to the thermodynamic integration point. Omitting anharmonic effects leads to the underestimation of the phonon contribution (Fig. 3).

EXPERIMENTAL DETAILS

Atom probe tomography (APT) samples were prepared in a dual-beam focused ion beam/scanning electron microscopy workstation (FIB/SEM) (Helios NanoLab 600^{TM}, FEI Company, USA) by the standard lift-out technique [12]. Laser Pulsed APT was carried out with a LEAP^{TM} 3000X HR (CAMECA) at a repetition rate of 200 kHz, a specimen temperature of about 60 K, a pressure lower than 1×10^{-10} Torr (1.33×10^{-8} Pa), and a laser pulse energy of 0.5 nJ. The evaporation rate of the specimen was 5 atoms per 1000 pulses. The positions and the time-of-flight of the ions coming into the detector are used to generate a three-dimensional reconstruction with IVAS^{TM}3.6.6 software (CAMECA). The accuracy of atomic-scale of APT and concentration are discussed in literature [13–16]. Previous results demonstrate that it is now possible to obtain highly quantitative information from APT.

[1] B. Grabowski, L. Ismer, T. Hickel, and J. Neugebauer, Phys. Rev. B **79**, 134106 (2009).
[2] A. Zunger, S.-H. Wei, L. G. Ferreira, and J. E. Bernard, Phys. Rev. Lett. **65**, 353 (1990).
[3] P. E. Blöchl, Phys. Rev. B **50**, 17953 (1994).
[4] G. Kresse and J. Hafner, Phys. Rev. B **48**, 13115 (1993).
[5] G. Kresse and J. Furthmüller, Phys. Rev. B **54**, 11169 (1996).
[6] G. Kresse and J. Furthmüller, Comput. Mater. Sci. **6**, 15 (1996).
[7] G. Kresse and D. Joubert, Phys. Rev. B **59**, 1758 (1999).
[8] S. Nosé, Mol. Phys. **52**, 255 (1984).
[9] H. J. Monkhorst and J. D. Pack, Phys. Rev. B **13**, 5188 (1976).
[10] D. Frenkel and B. Smit, *Understanding Molecular Simulation: From Algorithms to Applications*, Computational science series (Elsevier Science, 2001).
[11] G. Lehmann and M. Taut, Phys. Status Solidi B **54**, 469 (1972).
[12] K. Thompson, D. Lawrence, D. J. Larson, J. D. Olson, T. F. Kelly, and B. Gorman, Ultramicroscopy **107**, 131 (2007).
[13] D. N. Seidman, Annu. Rev. Mater. Res. **37**, 127 (2007).
[14] J. E. Allen, E. R. Hemesath, D. E. Perea, J. L. Lensch-Falk, Z. Li, F. Yin, M. H. Gass, P. Wang, A. L. Bleloch, R. E. Palmer, and L. J. Lauhon, Nat. Nanotechnol. **3**, 168 (2008).
[15] Y.-J. Kim, J. D. Weiss, E. E. Hellstrom, D. C. Larbalestier, and D. N. Seidman, Appl. Phys. Lett. **105**, 162604 (2014).
[16] A. Biswas, D. J. Siegel, and D. N. Seidman, Acta Mater. **75**, 322 (2014).